

# The Effects of External Magnetic Field on the Physical Properties of $\text{La}_{0.41}\text{Ca}_{0.59}\text{Mn}_{1-x}\text{Cu}_x\text{O}_3$ with $x = 0.06$ and $0.15$ in the Temperature Range of $100 - 300$ K

Y.E. Gunanto<sup>1\*</sup>, W.A. Adi<sup>2</sup>, B. Kurniawan<sup>3</sup>, A. Purwanto<sup>4</sup>, T. Ono<sup>5</sup>, H. Tanaka<sup>6</sup> and E. Steven<sup>7</sup>

<sup>1</sup>Dept. of Physics Education, University of Pelita Harapan, Karawaci, Tangerang 15811, Indonesia

<sup>2</sup>Center for Science and Technology of Advanced Materials, National Nuclear Energy Agency, Puspiptek Area Serpong, Tangerang Selatan 15310, Indonesia

<sup>3</sup>Dept. of Physics, University of Indonesia, Depok, 16424, Indonesia

<sup>4</sup>Dept. of Physics, STKIP Surya, Tangerang 15811, Indonesia

<sup>5</sup>Department of Physics, Osaka Prefecture University, Sakai, Osaka 599-8531, Japan

<sup>6</sup>Department of Physics, Tokyo Institute of Technology, Meguro-ku, Tokyo 152-8551, Japan

<sup>7</sup>Dept. of Physics, National High Magnetic Field Lab., Tallahassee, Florida, USA

## ARTICLE INFO

### Article history:

Received 12 November 2017

Received in revised form 17 January 2019

Accepted 24 January 2019

### Keywords:

$\text{La}_{0.41}\text{Ca}_{0.59}\text{Mn}_{1-x}\text{Cu}_x\text{O}_3$

External magnetic field

Crystal structure

Resistivity

Specific heat

## ABSTRACT

This work investigated the crystal structure, resistivity and specific heat of  $\text{La}_{0.41}\text{Ca}_{0.59}\text{Mn}_{1-x}\text{Cu}_x\text{O}_3$  with  $x = 0.06$  and  $0.15$ . The samples were prepared by a solid reaction method and in milling with high energy milling (HEM) of 700 rpm for ten hours. Neutron scattering with high resolution powder diffraction (HRPD) is used to analyze the phase and crystal structure. For resistivity analysis, four point probes are used, and SQUID Quantum Design is used for specific heat analysis in temperatures range of  $100 - 300$  K. In all cases, the sample has an orthorhombic crystal structure with a space group  $Pnma$ . The influence of a magnetic field on the specific heat and resistivity is also determined as a function of temperature. The resistivity increases in the presence of an external magnetic field. At the temperature less than  $184$  K, the resistivity follows the Arrhenius model ( $\ln R$  varies as  $1/T^{0.25}$ ) while at higher temperatures it fits the metal-semiconductor model ( $\ln R$  varies as  $1/T$ ). The electronic specific heat parameter  $\gamma$  varies with magnetic field at  $x = 0.06$ , but not at  $x = 0.15$ .

© 2019 Atom Indonesia. All rights reserved

## INTRODUCTION

Manganites of rare earth with the general formula  $\text{RE}_{1-x}\text{AE}_x\text{MnO}_3$ , where RE are rare earth ions with three valences, e.g. La, Pr, Gd etc. and AE = alkaline earth alkaline ions, e.g. Ca, Ba, Sr etc. are still intensively studied. Works focusing on various physical properties of the compounds, such as magnetoresistance (MR), crystal structure change, metal-insulator transition, specific heat, large magneto-caloric effect, and high electrical conductivity have been reported [1-16]. These rare

earths manganite compounds have found a wide range of application, such as a mild hyperthermia mediator [1], magnetic refrigeration technology near room temperature [5], and a fuel cell cathode [7-9].

Until now, the results of measurements and analysis of this material still make a lot of differences. Suppose  $\text{La}_{1-x}\text{Sr}_x\text{MnO}_3$  will change from orthorhombic ( $x < 0.2$ ) to rhombohedral ( $x > 0.2$ ) [1], at low temperatures,  $\text{La}_{1-x}\text{Ca}_x\text{MnO}_3$  structure will change from cubic to rhombohedral then to orthorhombic [2], while  $\text{La}_{0.65}\text{Ca}_{0.35-x}\text{Ba}_x\text{MnO}_3$  has a rhombohedral crystal structure for  $x < 0.15$  and a cubic for  $0.15 < x < 0.25$  [3]. The resistivity will decrease with the presence of an external magnetic field and a metal-insulator transition temperature

\* Corresponding author.

E-mail address: [yohanes.gunanto@uph.edu](mailto:yohanes.gunanto@uph.edu)

DOI: <https://doi.org/10.17146/aij.2019.769>

( $T_{MI}$ ) of about 243 K. In case of  $T > T_{MI}$ , the resistivity as a function of temperature could be described by two different models, namely the variable range hopping (VRH) model or Arrhenius model and the adiabatic small polaron hopping (ASPH) model but more in line with the second model (ASPH). The same results are also obtained by S. O. Manjunatha *et al.* [3], for  $T > T_{MI}$  samples more suited to adiabatic small polaron hopping (ASPH) model [6]. Z. Han *et al.* found that the influence of the external magnetic field  $H$  is not proportional to the value of the electronic specific heat coefficient  $\gamma$ . If the value of  $H$  is greater, then the  $\gamma$ -coefficient value may rise and fall. This condition occurs when compared to the  $\gamma$ -coefficient values without an external magnetic field [15].

In this work, the authors will analyze the influence of the valence of the Mn- and Cu sites on the crystal structure of  $La_{0.41}Ca_{0.59}Mn_{1-x}Cu_xO_3$  compound ( $x = 0.06$  and  $0.15$ ), both at room temperature and at low temperatures using high resolution neutron scattering in BATAN Serpong. Next, the authors present an analysis on the influence of an external magnetic field on the resistivity values employing the four point probe method and on the specific heat values by employing the SQUID Quantum Design method. Both measurements are carried out in the temperature range of 100 - 300 K.

### EXPERIMENTAL METHODS

The  $La_{0.41}Ca_{0.59}Mn_{1-x}O_3$  sample was prepared by thoroughly mixing stoichiometric amounts of  $CaCO_3$ ,  $La_2O_3$ , and  $MnO_2$  with at least 99.9 % purity. The mixed powders were ballmilled for five hours, heated at 1350 °C for six hours, then repeat the ballmill process for another ten hours and heated at 1100 °C for twenty-four hours [17]. The neutron-powder-diffraction experiments

were performed with a high-resolution powder diffractometer HRPD ( $\lambda=1.8223 \text{ \AA}$ ) at the Neutron Scattering Center of BATAN, Serpong, Indonesia. The sample of about four grams was loaded in a cylindrical vanadium can and placed in a helium cryostat. The data was collected in the angular range of  $2\theta = 2.5^\circ - 157^\circ$  with an angular interval of  $0.05^\circ$  for the room temperature measurement and with an angular interval of  $0.2^\circ$  for the 18 K measurement. The data reduction was performed after the measurement. The diffraction patterns were analyzed using the Rietveld refinement program FULLPROF, which can refine the magnetic structure along with the crystallographic structure.

Four point probes are used to characterize resistivity as a function of temperature and magnetic fields at the Magnetic Lab. Florida University USA. The sample has dimensions of ~ 7 mm and width of ~ 3 mm.

The specific heat was measured in the temperature range of 100-300 K in the magnetic field with the range of 0-9 T using the SQUID Quantum Design at Tanaka Lab. Tokyo Institute of Technology Tokyo Japan [18].

### RESULTS AND DISCUSSION

The diffraction pattern of the measurement result using high resolution powder diffraction (HRPD) at room temperature for  $x = 0.06$  and  $0.15$  stoichiometry is shown in Fig. 1. The results of the analysis using the FULLPROF program show that both samples were single phase and the diffraction lines could be indexed with an orthorhombic  $Pnma$  space group. Similar results were obtained by Y. Bitla *et al.* [13] and M. L. Wu *et al.* [14], i.e. Crystals have an orthorhombic structure. The full results are presented in Table 1.

**Table 1.** Parameters at room temperature for Cu = 0.06 and 0.15.

x	Parameters					atom	Atoms Position					$\chi^2$
	a (Å)	b (Å)	c (Å)	$\alpha = \beta = \gamma$	V (Å) <sup>3</sup>		X	Y	Z	B	Occ.	
0.06	5.4209	7.6332	5.4385	90	225.04	La <sup>3+</sup>	-0.02234	0.25000	0.00012	0.35176	1.63022	1.15
						Ca <sup>2+</sup>	-0.02234	0.25000	0.00012	0.35176	2.36977	
						Mn <sup>4+</sup>	0.00000	0.00000	0.50000	0.10000	3.77122	
						O <sup>2-</sup> (1)	0.50234	0.25000	-0.05817	0.87820	3.85119	
						O <sup>2-</sup> (2)	0.27480	-0.03191	-0.27727	1.43568	8.23294	
Cu <sup>2+</sup>	0.00000	0.00000	0.50000	0.10000	0.22878							
0.15	5.4328	7.6592	5.4469	90	226.65	La <sup>3+</sup>	-0.01088	0.25000	0.00535	0.35176	1.82770	1.58
						Ca <sup>2+</sup>	-0.01088	0.25000	0.00535	0.35176	2.17229	
						Mn <sup>4+</sup>	0.00000	0.00000	0.50000	0.10000	3.89600	
						O <sup>2-</sup> (1)	0.50781	0.25000	-0.05947	0.87820	3.94898	
						O <sup>2-</sup> (2)	0.27823	-0.03048	-0.27515	1.43568	8.60244	
Cu <sup>2+</sup>	0.00000	0.00000	0.50000	0.10000	0.69030							

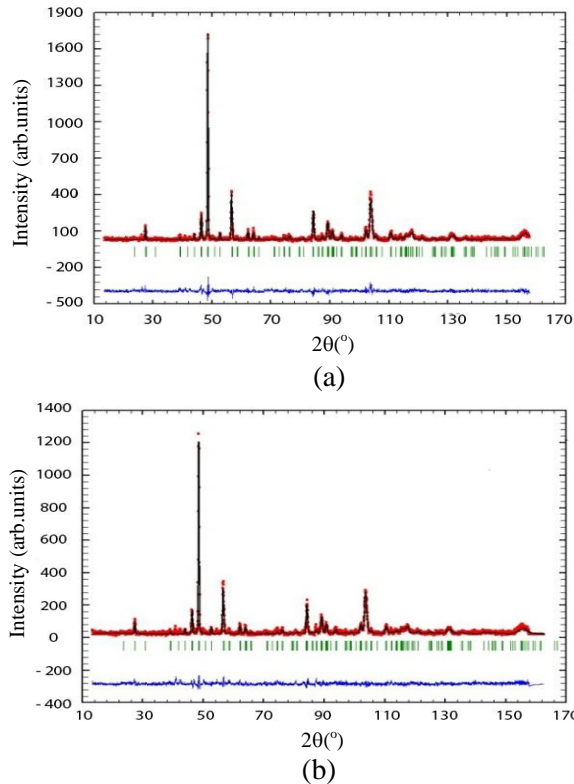


Fig. 1. The diffraction pattern at room temperature for (a) Cu = 0.06 and (b) Cu = 0.15.

Although there are no changes in the crystal structure either at room temperature or at low temperature of 18 K, a change is observed in the value of the lattice parameter, in this case the *b* parameter and the volume *V*. The diffraction pattern at low temperature of 18 K for Cu = 0.06 is presented in figure 2. These results are listed in table 2. These changes are related to the Jahn-Teller effect, therefore the crystals are distorted or deformed [17].

Table 2. Parameters at room temperature and low temperature for Cu = 0.06.

	Parameters					$\chi^2$
	<i>a</i> (Å)	<i>b</i> (Å)	<i>c</i> (Å)	$\alpha = \beta = \gamma$	<i>V</i> (Å) <sup>3</sup>	
300 K	5.4209	7.6332	5.4385	90	225.04	1.15
18 K	5.4341	7.5394	5.4602	90	223.70	2.16

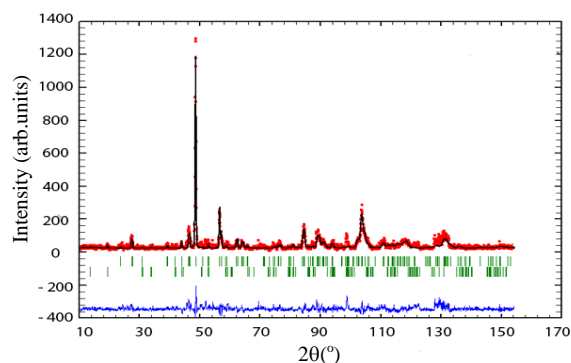


Fig. 2. The diffraction pattern at room temperature for Cu = 0.06 at 18 K.

Figure 3 shows the resistivity as a function of temperature, both are without the presence of an external magnetic field and under the presence of an external magnetic field. It appears that if Cu content increases, the sample resistivity also increases. The value of resistivity will increase with the presence of an external magnetic field. The samples have positive magnetoresistance, the value of resistivity is greater in the presence of an external magnetic field.

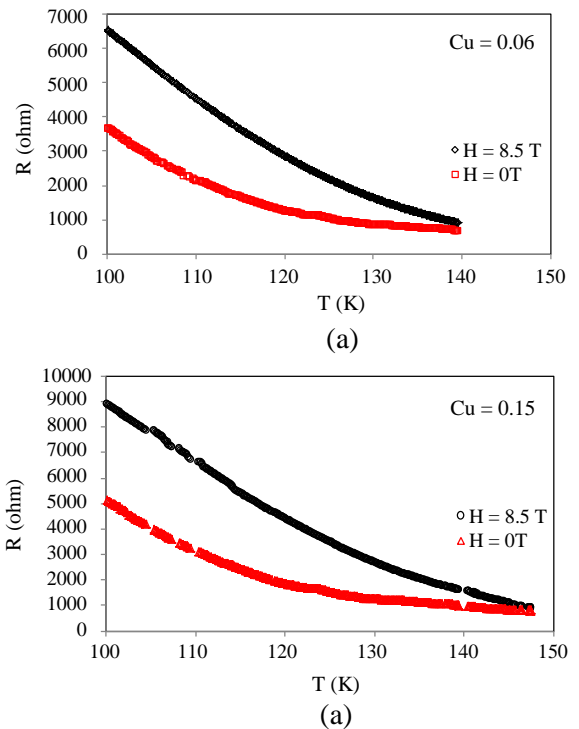


Fig. 3. Resistivity as a function of temperature without an external magnetic field and with an external magnetic field of 8.5 T for (a) Cu = 0.06 and (b) Cu = 0.15.

The relation between resistivity and temperature is expressed as an exponential dependence. The high temperature regime can be analyzed using two models i.e. the adiabatic small polaron hopping (ASPH) model and variable range hopping (VRH) model [3]. The ASPH model is given by relation,

$$R(T) = C \exp(E_a/kT) \tag{1}$$

where *R* is the electrical resistance, *C* is a constant, *E<sub>a</sub>* is activation energy, *k* is Boltzmann's constant, and *T* is absolute temperature. On the other hand, the variable range hopping (VRH) is given by relation [3],

$$R(T) = C \exp(T_0/T)^{1/4} \tag{2}$$

The activation energies, *E<sub>a</sub>* at *H* = 0 T and *H* = 8.5 T are found to be  $8.9 \times 10^{-6}$  eV and  $1.3 \times 10^{-5}$  eV, respectively, according to equation (1) [19].

In Figs. 4 and 5, at temperatures greater than 184 K, for Cu content of either 0.06 or 0.15, the samples' electrical resistance behaviour is more suited to the metal-semiconductor model ( $\ln R - 1/T$ ), whereas for temperatures less than 184 K the samples' electrical resistance is more in tune with the Arrhenius model (VRH) ( $\ln R - 1/T^{0.25}$ ).

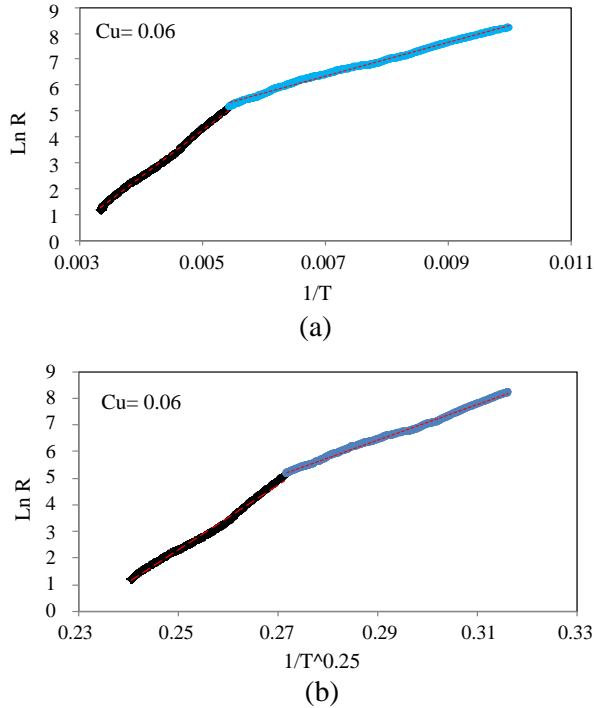


Fig. 4. (a) Graph R to  $1/T$  and (b) Graph R to  $1/T^{0.25}$  for sample Cu = 0.06.

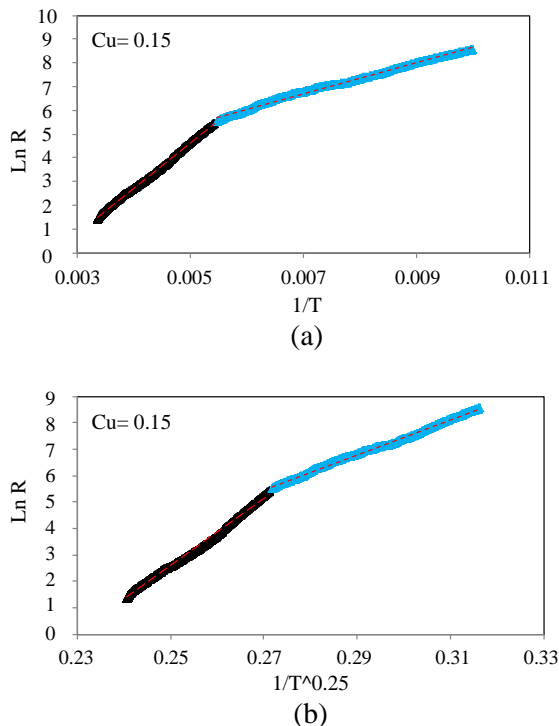


Fig. 5. (a) Graph  $\ln R$  to  $1/T$  and (b) Graph  $\ln R$  to  $1/T^{0.25}$  for sample Cu = 0.15.

The effect can be explained by considering the presence of Cu ions, in which Cu ions can exist in two states, namely  $\text{Cu}^{2+}$  ( $\sim 0.73 \text{ \AA}$ ) and  $\text{Cu}^{3+}$  ( $\sim 0.54 \text{ \AA}$ ). Similarly, Mn ions can be  $\text{Mn}^{3+}$  ( $\sim 0.645 \text{ \AA}$ ) and  $\text{Mn}^{4+}$  ( $0.53 \text{ \AA}$ ), therefore when the La ions with three valences ( $\text{La}^{3+}$ ) are substituted by the Cu ions with two valences ( $\text{Cu}^{2+}$ ), this course will introduce a hole in the Mn sites [19].

At higher Cu-doping, smaller  $\text{Cu}^{3+}$  ions are dominant, thus reducing the internal chemical pressure and effectively increasing the resistance. On the contrary, at lower Cu-doping concentrations,  $\text{Cu}^{2+}$  ions that are larger than the  $\text{Mn}^{3+}$  are the dominant factors, inducing internal chemical pressure [20] which in turn lower the resistance of the sample. Moreover, the Cu-doping can reduce the  $\text{Mn}^{3+} (3d^4, t_{2g}^3 e_g^1) - \text{Mn}^{4+} (3d^3, t_{2g}^3 e_g^0)$  ratio, therefore reducing the double exchange interaction, and the number of both the hopping electrons and the sites [21].

To calculate the specific heat, one could use the equation:

$$C(T) = \gamma T + \beta_3 T^3 + \beta_5 T^5 + \delta T^n + \alpha T^{-2} \quad (3)$$

where  $\gamma T$  is the electronic contribution to the specific heat,  $\beta_3 T^3$  and  $\beta_5 T^5$  is the phonon contribution to the specific heat,  $\delta T^n$  is the spin wave (antiferromagnetic) component of the specific heat, and  $\alpha T^{-2}$  is the hyperfine structure contribution to the specific heat. The plot of the specific heat as a function of temperature  $C(T)$  without an external magnetic field or with an external magnetic field of 9 T is reported in Fig. 6. For larger Cu content and the presence of an external magnetic field, the specific heat sample will be larger for that same temperature. The external magnetic field also affects the values of specific heat parameters, electronic, phonon, and spin wave. It appears that the values of these parameters will change with the presence of an external magnetic field. The summary of the results is listed in Table 3.

Table 3. List of Specific Heat Coefficient Parameters both with no external magnetic field and Under the influence of an external magnetic field.

Cu	$H(T)$	$\gamma (\text{mJ} \cdot \text{mol}^{-1} \cdot \text{K}^{-2})$	$\delta (\text{J} \cdot \text{mol}^{-1} \cdot \text{K}^{-3})$
0.06	0	$23.03 \times 10^{-1}$	$1.66 \times 10^{-2}$
	9	$17.28 \times 10^{-1}$	$1.36 \times 10^{-2}$
0.15	0	$23.03 \times 10^{-1}$	$1.66 \times 10^{-2}$
	9	$23.22 \times 10^{-1}$	$1.64 \times 10^{-2}$

Based on the results listed in Table 3, for  $H = 0 \text{ T}$  and for more Cu content, then the quantities in the specific heat are relatively constant only the

$\gamma$ -coefficient value slightly increases. However, for  $H = 9$  T, the external magnetic field becomes very influential on the  $\gamma$  and the  $\delta$  coefficients' values, while the values of the other constants are relatively small and unchanged.

The effect of an external magnetic field ( $H$ ) on the samples with an  $x = 0.06$  stoichiometry is that the value of the  $\gamma$ -coefficient has the most significant change compared to the other constants. While for the  $x = 0.15$  samples, the influence of an external magnetic field seems to be most significant on the value of the  $\beta$ -coefficient.

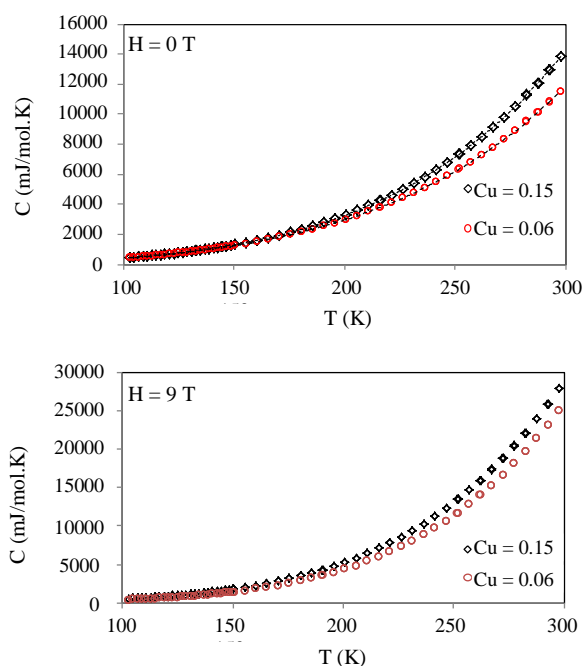


**Fig. 6.** The specific heat as a temperature function for samples with  $\text{Cu} = 0.06$  and  $0.15$  without and with an external magnetic field of  $9$  T.

Our finding shows that the coefficient of the electronic specific heat ( $\gamma$ ) has reached the value of  $2.3 \text{ mJ}\cdot\text{mol}^{-1}\cdot\text{K}^{-2}$  in the absence of an external magnetic field. This result is not much different from that obtained by L. Ghivelder *et al.* [22] which is about  $3 \text{ mJ}\cdot\text{mol}^{-1}\cdot\text{K}^{-2}$ . The specific heat of both samples does have similarities, as is expected based upon their identical crystal structure [2].

## CONCLUSION

At room temperature and low temperature of  $18$  K, the orthorhombic space group crystal structure of the  $\text{La}_{0.41}\text{Ca}_{0.59}\text{Mn}_{1-x}\text{Cu}_x\text{O}_3$  for  $x = 0.06$  and  $0.15$  has not experienced any alterations. The differences in the lattice parameters are insignificant.

The presence of an external magnetic field resulted in the increase of the resistivity of the sample, so it is a positive magnetoresistance. As for

the specific heat quantity, the external magnetic field affects the value of its parameters, particularly the electronic specific heat constant and the specific heat of the phonon constants.

## ACKNOWLEDGMENT

We are grateful for the support and facilities provided by BATAN (National Nuclear Energy Agency), and Tanaka Lab. for Low Temperature, Tokyo Institute of Technology Japan. A portion of this work was carried out at National High Magnetic Field Laboratory.

## REFERENCES

1. K. McBride, J. Cook, S. Gray *et al.*, *CrystEngComm* **18** (2016) 407. DOI: 10.1039/C5CE01890K
2. M. Pissas and D. Koumoulis, *J. Appl. Phys.* **122** (2017) 143902.
3. S.O. Manjunatha, A. Rao, T.-Y. Lin, *et al.*, *J. Alloys Compd.* **619** (2015) 303.
4. H. Baaziz, N.K. Maaloul, A. Tozri *et al.*, *Chem. Phys. Lett.* (2015). <http://dx.doi.org/10.1016/j.cplett.2015.10.012>
5. F. Ayadi, Y. Regaieg, W. Cheikhrouhou-Koubaa *et al.*, *J. Magn. Magn. Mater.* **381** (2015) 215.
6. S.O. Manjunatha, A. Rao, Subhashini *et al.*, *J. Alloys Compd.* **640** (2015) 154.
7. C. Marinescu, L. Vradman, S. Tanasescu *et al.*, *J. Solid State Chem.* **230** (2015) 411.
8. E. Olsson, X. Aparicio-Anglès and N.H. De Leeuw, *J. Chem. Phys.* **145** (2016) 014703.
9. L. Navarrete, M. Balaguer, V.B. Vert *et al.*, *J. Electrochem. Soc.* **163** (2016) F1440.
10. N. Erdenee, U. Enkhnanan, S. Galsan *et al.*, *Journal of Nanomaterials* **2017** (2017) 8. <https://doi.org/10.1155/2017/9120586>.
11. Y. Shlapa, S. Solopan, A. Bodnaruk *et al.*, *Nanoscale Research Letters* **12** (2017) Doi 10.1186/s11671-017-1884-4.
12. M. Mihalikjr, Z. Jaglicic, M. Fitta, V. Kavecansky *et al.*, arXiv:1605.05128v2 [cond-mat.mtrl-sci] (17 Jun 2016).
13. Y. Bitla and S.N. Kaul, *Europhysics Journal Exploring* **103** 57010 (2013). Doi: 10.1209/0295-5075/103/57010.

14. M.L. Wu, C.P. Yang, D.W. Shi *et al.*, AIP Advances **4** (2014) 047123.
15. Z. Han and Z. Jing, Advances in Condensed Matter Physics **2014**, Article ID 394296, <http://dx.doi.org/10.1155/2014/394296>
16. A.A. Hendi, I.A.A. Latif, and S.A. saleh, Journal of American Science **7** (2011).
17. Y.E. Gunanto, E. Steven, B. Kurniawan *et al.*, IOP Conf. Series: Materials Science and Engineering **202** (2017). Doi:10.1088/1757-899X/202/1/012075
18. Y.E. Gunanto, B. Kurniawan, W. Nursiyanto *et al.*, Indonesia Journal Materials of Science **12** (2011) 220.
19. Y.E. Gunanto, W.A. Adi, B. Kurniawan *et al.*, International Journal of Technology **1** (2017) 1117.
20. P. Kumar and R.K. Dwivedi, J. the Korean Physical Society **58** (2011) 58.
21. M.S. Kim, J.B. Yang, P.E. Paris *et al.*, J. Applied Physics **97** (2005) 1.
22. L. Ghivelder, I.A. Castillo, N.M. Alford *et al.*, J. Magn. Magn. Mater. **189** (1998) 274.